https://doi.org/10.1007/s41230-019-8127-5

Mixed regulation model of ceramic particles with molten high-chromium iron KmTBCr26

***Qi Dong, Shu-ming Xing, and Bo Qiu**

School of Mechanical, Electronic and Control Engineering, Beijing Jiaotong University, Beijing 100080, China

Abstract: Particle reinforced metal matrix composites have many problems such as complicated preparation process, high production costs, weak interface bonding between the ceramic and metal matrix, uneven distribution of ceramic particles and so on. To solve these problems, the method of "shoot mixing + pressure compositing" (SM-PC) and a mixed regulation model of ceramic particles with molten steel were proposed. In the shoot mixing process, the special designed die casting equipment was used to make the particles with the molten metal mixed in the runner at a certain ejection speed (150 $mm \cdot s^{-1}$). After the mixture is filled with the mold, the pressure is maintained until the end of solidification. In order to optimize this method to obtain the more uniform particle distribution, the parameters (ejection speed, preheating temperature of particles, the shape and size of runner) in the model were selected for sample preparation. Taking the distribution index of particles as the evaluation criterion, it is concluded that the uniform distribution of particles can be promoted with the increase of ejection velocity, the increase of particle preheating temperature, and the small change of gate size. When the preheating temperature of particles was 1,100 °C, and the shape of the runner was trumpet, the optimal particle distribution composite parts was obtained. Meanwhile, the particles and the matrix achieved strong interface bonding – "Class I interface " under the pressure compositing, even though they're non-wetting.

Key words: ceramic particles; Cr26; SM-PC; particle distribution; interface

CLC numbers: TG143.1 **Document code:** A **Article ID:** 1672-6421(2019)02-135-06

Adding large-size (mm) particles into an alloy can improve the abrasion resistance[1]. Subsequently, researches on particle reinforced aluminum alloy composites confirmed that the particles with a size approaching mm-scale can effectively lower the wear rate and does better than the micron particle[2–3]. The service life of Zirconia Toughened Alumina (ZTA, 1–5 mm) reinforced high-chromium cast iron produced by MAGOTTEAU Xin Belgium is 3–5 times longer than that of iron with no compound [4–5].

Liquid-solid complex method (liquid method or casting method) is the most widely-used for the preparation of many composite materials[6]. Sree Manu K M[7] obtained better separation, dispersion and distribution of the microsilica particles in the solidified matrix by the compocasting cum squeeze casting process than by liquid metal stir casting. Dhanashekar M[8] found the squeeze casting and ceramic particle can reduce the porosity and increase the wear resistance of aluminum matrix composites. Although this method is easy to operate, the distribution of large-size (mm) particles are not uniform because the homogeneous ceramic/metal mixture can be separated by gravity during the pouring and filling process.

The wettability, stability and solubility of ceramic particles in molten metal are the keys to preparing the composite[9]. Using alloying additions or ceramic surface metallization method can make a non-wetting complex system become a wetting system, and improve the distribution and interface bonding strength[10–12]. However, pretreated particles are not favored for the production of composite materials, due to the high cost mainly caused by the complex process.

A new method for preparing liquid die forging composite material is proposed using the strategy of mixed flow and high pressure composite[13]. In the process of flowing into the cavity, the liquid metal

***Qi Dong**

Female, born in 1987, Ph.D. Her research interests mainly focus on wear resistant metal materials.

E-mai: 15116360@bjtu.edu.cn

Received: 2018-10-10; Accepted: 2018-12-28

was added with the particles, to achieve the "with mixed flow" (shoot mixing), and to form the solid-liquid mixed flow; under the pressure, the particles get into the cavity; during the next action of high pressure, strengthening body and matrix solid were tightly combined, followed by a rapid solidification, to achieve the "high pressure compositing".

By establishing a mixed regulation model, the mechanism and conditions of mixing ceramic particles with the metal melt were studied based on the principle of thermodynamics. Discussion was also engaged on the relationship between process parameters (mixing speed, mixing temperature), sprue geometric characteristics and the thermal physical characteristics of metal.

1 Modeling

1.1 Fundamental assumptions

Before the mixing, the ceramic particles (spherical particles with a radius of r) connect with each other. The particles move at a constant speed V_p under the temperature of T_p, and the liquid metal moves at a constant speed V_m under T_m along the equal cross section.

As shown in Fig. 1, in the mixing process, it is assumed that there is no chemical reaction between liquid metal and ceramic at mixture temperature T_{mix}, because the model limits the range of application between non-wetted particles and molten metal, and the chemical reaction can lead to wettability change in the

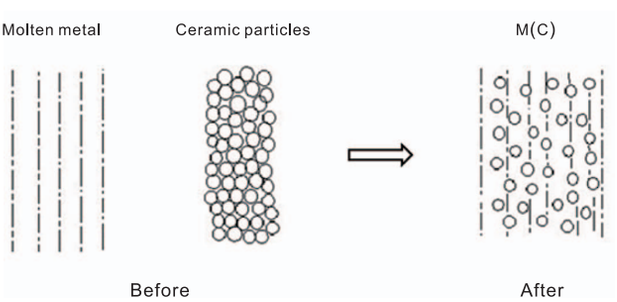

Fig. 1: Simplified graph of mixing process

mixing process. The mixing is an isobaric process, therefore it can be assumed that the pressure of the system before and after the mixing is constant.

After the mixing, the relative velocity of liquid metal and particle becomes 0, and the velocity of the mixture is V_{mix}. There is no contact among adjacent ceramic particles, and the liquid metal is filled among those ceramic particles.

1.2 Temperature and speed of mixture

According to the principle of thermal equilibrium, there is no internal heat source mixing process. After the mixing, the temperature T_{mix} is as follows:

$$T_{mix} = \frac{C_{mix}\Delta T_{ls} T_{mix0} + qf_m T_l}{C_{mix}\Delta T_{ls} + qf_m} \tag{1}$$

where C_{mix} is the weighted specific heat of mixtures, ΔT_{ls} is crystallization temperature range of molten metal, q is the metal solidification latent heat, f_m is the liquid metal fraction. Referring to the combined motion of the molten metal and the particles after the mixing, it is assumed that the velocity before and after mixing obeys the kinematics principle, V_{mix} can be obtained from the equation (2):

$$V_{mix} = \frac{f_{sm}}{S_0(1-f)(1-\lambda)} V_m \tag{2}$$

where V_m is the liquid metal velocity, f_{ms} is the solid fraction, q is the metal solidification latent heat, λ_{is} the porosity of particles.

1.3 Hybrid drive ΔG_{mix}

Gibbs functions can be added depending on the Mixture Law:

$$\Delta G_{mix} = X_m \Delta G_m + X_p \Delta G_p \tag{3}$$

where X_p is the particle weight fraction, X_m is the metal weight fraction.

1.3.1 Gibbs free energy of particles

The Gibbs free energy of particles (ΔG_p) includes three parts, i.e. the enthalpy change caused by the change of temperature, the enthalpy change caused by the change of configuration entropy, and the energy change (ΔU_p) caused by the particle interface changing from solid-gas state to solid-liquid state. The mixing entropy of particles (ΔS_p) can be obtained according to the Boltzmann equation [14].

$$\Delta G_p = \Delta U_p - T_{mix}\Delta S_p - S_p \Delta T = -4n\pi r^2 \sigma_{gl}\cos\theta_{mp} - T_{mix}k\left(\frac{V_m(1-\lambda)}{4/3\pi r^3}\ln\frac{V_m(1-\lambda)}{1-\lambda+f} + \frac{V_m f(1-\lambda)}{4/3\pi r^3(1-f)}\ln\frac{f}{1-\lambda+f}\right) \tag{4}$$

1.3.2 Gibbs free energy of metal

$$\Delta G_m = \frac{f_{ms} q(T_{mix} - T_m)}{T_l} + \sigma_{gl}\Delta A_{sur} - 3\frac{V_m f(1-\lambda)}{r(1-\lambda)}\sigma_{gl}\cos\theta_{mp} - f_p A_{mc}\sigma_{gl}\cos\theta_{mc} \tag{5}$$

where A_{mc} is the cross-sectional area, ΔA_{sur} is the surface area change before and after the liquid metal, σ_{gl} is the liquid metal surface tension, $\cos\theta_{mp}$ is wetting angle between metals and ceramics, and $\cos\theta_{mc}$ is the metal liquid cavity wall wetting angle.

1.3.3 System Gibbs free enthalpy variation of pre- and post-mixing

Substitute equations (4) and (5) into equation (3). In order to simplify the formula for discussion, the part of the formula is denoted as A which is greater than 0, and the others are B:

$$\Delta G_{mix} = A + B \tag{6}$$

1.4 Condition of flow mixing in non-wetting system

When $\cos\theta_{mc} < 0$, $\cos\theta_{mp} < 0$

$$A = \sigma_{gl}\left\{\left(1-\frac{f_p p_m}{p_p - f_p p_p}\right)\Delta A_{sur} - 3\frac{V_{mf}(1-\lambda)}{r(1-\lambda)}\sigma_{gl}\cos\theta_{mp} - \left(1-\frac{f_p p_m}{p_p - f_p p_p}\right) f_p A_{mc}\sigma_{gl}\cos\theta_{mp}\right\} > 0 \quad (7)$$

where A is the resistance term of mixing; the smaller the absolute value of A, the more favorable to mixing. The main factors contributing to the reduction of A are: the smaller the $\sigma_{gl}/r\Delta A_{sur}$/wetting angle between metals and ceramics $\cos\theta_{mp}$, the larger the particle radius r.

$$B = \left(1-\frac{f_p p_m}{p_p - f_p p_p}\right)\left\{\frac{(T_l - T_{mix})(T_{mix} - T_m)}{\Delta T_{ls} T_l} q\right\} - \frac{f_p p_m}{p_p - f_p p_p} \left\{T_{mix} k\left(\frac{V(1-\lambda)}{4/3\pi r^3}\ln\frac{V_m(1-\lambda)}{1-\lambda+f} + \frac{V_m f(1-\lambda)}{4/3\pi r^3(1-f)}\ln\frac{f}{1-\lambda+f}\right) + C_p \ln\frac{T_{mix}}{T_p}(T_{mix} - T_p)\right\} + \frac{1}{2}\left[M_p(V_{mix}^2 - V_p^2) + M_m(V_{mix}^2 - V_m^2)\right] < 0 \quad (8)$$

where B is a driving force of mixing, and promotes the combination of factors as follows: the smaller the particle fraction f_p; the higher the initial temperature of molten metal and ceramic particles T_m and T_p; the greater the molten metal speed V_m. In terms of materials, the alloy with great crystallization latent heat ΔT_{ls} and low temperature range can be easy to mix.

Therefore, the lower the value of ΔG_{mix}, the easier the molten metal and ceramic particles mix. Based on the experimental results predicted by the mixed regulation model, the mixing patterns are prepared by the method of "shoot mixing+ pressure compositing" (SM-PC), and the mixing effects of the three parameters (V_m, T_p and ΔA_{sur}) are verified by experiments under the condition that the other parameters are not changed.

2 Experimental

2.1 Materials

In this work, high-chromium iron KmTBCr26 was selected as the matrix, and its composition is shown in Table 1. ZTA was selected as the enhancement phase, and its physical and mechanical properties are shown in Table 2. The average size of the particle was 2–4 mm, and the shape was irregular. The morphology of ZTA ceramic particles is shown in Fig. 2.

Table 1: Chemical compositions of KmTBCr26

Material	C	Si	Mn	Cr	Mo	W	Ni	P	S
ω (%)	2.8–3.0	0.8–1.0	1.8–2.0	25–27	0.7–1.0	0.9–1.3	0.3–0.5	⩽ 0.10	⩽ 0.06

Table 2: Physical and mechanical properties of ZTA

Density (g·cm^{-3})	Fracture toughness (MPa·M$^{1/2}$)	Bending strength (MPa)	Hardness (HV)	Coefficient of thermal expansion (*10^{-6})
4.2–4.6	7.0–8.0	500–600	1,400–1,600	7.7–9.0

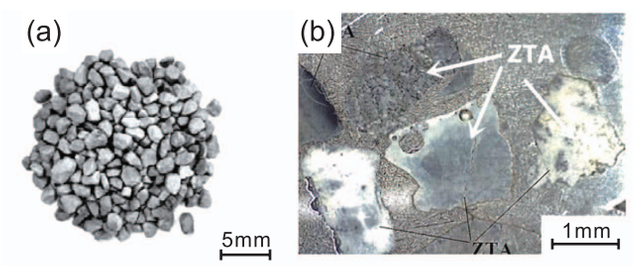

Fig. 2: (a) Exterior of ZTA ceramic particles; (b) Composite particle morphology

2.2 Specimen preparation

The preparation process of composite parts is shown in Fig. 3. The shoot mixing process in SM-PC was done with forging composite mold, which is shown in Fig. 4.

After the mixture flowed into the runner of the squeeze casting mold, it then filled in the composite part cavity with a

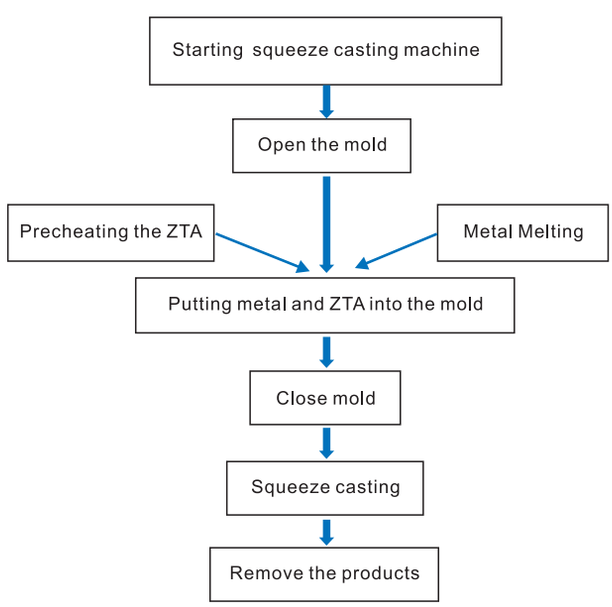

Fig. 3: Technological process of squeeze casting for composite anti-wear parts

size of 240 mm × 80 mm × 60mm. The cavity with two parts (A+B) shown in Fig. 5 were made at one time. Finally, the pressure compositing experiment was conducted by utilizing a vertical liquid die forging machine under fill pressure cylinder pressure.

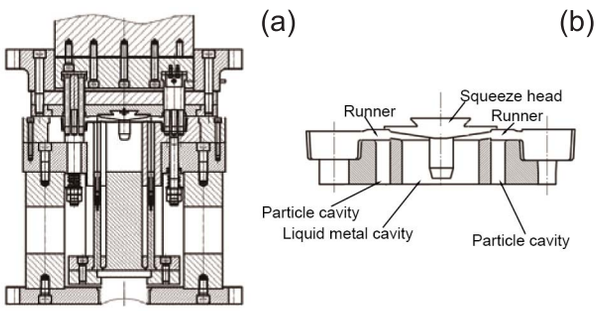

Fig. 4: (a) Mould assembly drawing of squeezing casting composite parts (b) Runner of squeeze casting mold

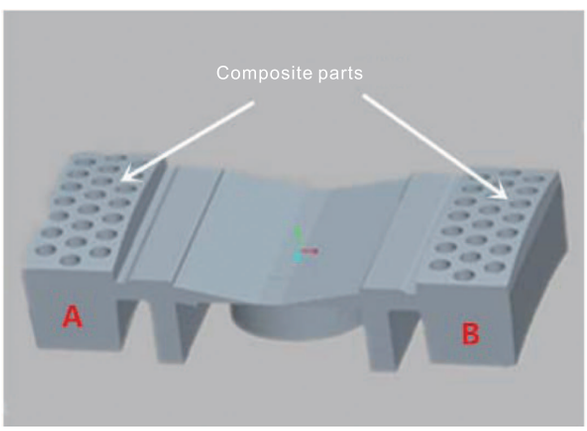

Fig. 5: Diagram of composite parts

2.3 Technological parameters

Table 3 shows the experimental parameters of the process:

Table 3: SM-PC technological parameters

Technological parameters	Data range
Ejection speed	50/150 mm·s^{-1}
Particle preheating temperature	0/1,100 °C
Pouring temperature	1,600 °C
Main cylinder pressure	700 t
Fill pressure cylinder pressure	500 t
Pack-out cylinder pressure	280 t
Pressure holding time	12 s
Mold preheating temperature	150–200 °C
Single composite part weight	2.2 kg

2.4 Inhomogeneity of particles

The composite samples can be evaluated by the distribution of particles in the metal matrix. Because of the macro-millimeter scale of particles, it is convenient to count the particles at different positions. Figure 6 shows the morphology and the cross-section of wear-resistant parts.

The samples were divided into three typical cross-sections of the inside, middle and outside, and each section includes top, center and bottom shown as Fig. 7. The mixing of particles with the metal matrix was observed with the naked eye (particle size > 5 mm) or magnifying glass with magnification of 10–30 times (particle size 1–5 mm). The total number of particles n of each observation surface was counted, and the area of the observed surface was measured. The average value of the measured results on both sides of each observation plane was taken as the mixing degree of the observed surface, which was calculated respectively i=1,2,3…,9 as Fig. 7 shows.

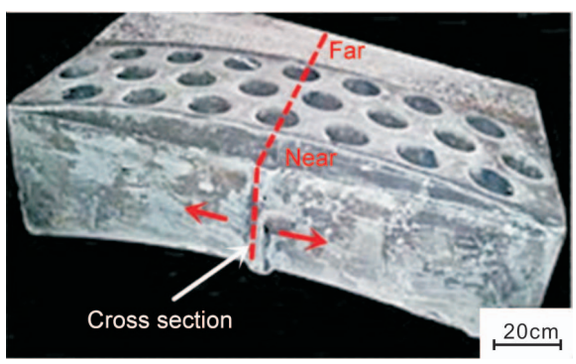

Fig. 6: Appearance of squeeze casting composite parts (240 x 80 x 60 mm^3)

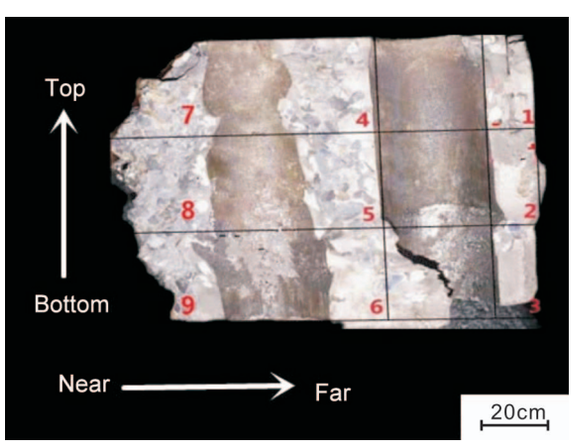

Fig. 7: Cross-section of squeeze casting composite parts

The average degree of mixing of the nine observation surfaces can be calculated by equation (9):

$$\overline{\zeta'}=\frac{1}{n}\sum_{i=1}^{n}\zeta_i' \tag{9}$$

The degree of mixing was calculated by $\zeta = z/a$, the number of particles z and the area a (cm^2) of each observation surface were counted by statistics, and the results were recorded as ζ_i (i = 1, 2, ..., 9). The value of deviation S is used to judge the inhomogeneity of particles. The smaller the deviation, the

more uniform the particle distribution. S can be calculated by equation (10):

$$S=\sqrt{\frac{1}{n-1}\sum_{i=1}^{N}(\zeta_i'-\overline{\zeta'}^{\,2})} \quad (10)$$

3 Results and discussion

3.1 Effect of ejection velocity on particle distribution

In the shoot mixing steps, metal liquids and ceramic particles are placed in the liquid metal chamber (sectional area A_m) and the particle chamber (sectional area A_p) at a predetermined ratio as equation (11) shows, and velocity is provided by the ejection velocity ($V_p = V$ = ejection velocity).

$$f_p = \frac{A_p}{A_m + A_p} \quad (11)$$

When the ejection velocity was relatively low (50 mm·s^{-1}), the mixture flowed to the proximal end of the cavity, resulting in a relatively small number of particles at the far end of the anti-wear part, while the near-end particles had a aggregation phenomenon, as shown in Fig. 8(a). The caluculated data indicate that S is obviously reduced to 2.87 from 3.51. When the steel fluid was advancing at a high speed, the flow resistance was small, and the mixture could rush to the far end of the cavity, as shown in Fig. 8(b). The results show that the upward velocity of the ejection should not be less than 150 mm·s^{-1}.

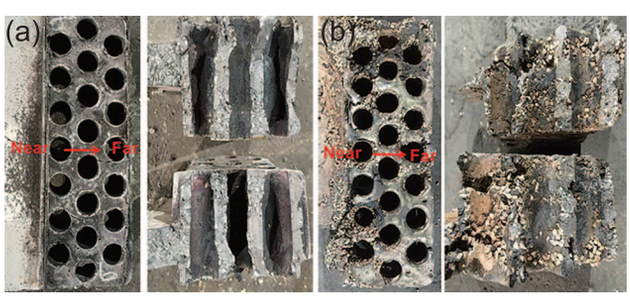

Fig. 8: Effect of speed on squeeze casting composite anti-wear parts: (a) 50 mm·s^{-1}; (b) 150 mm·s^{-1}

3.2 Effect of T_P on particle distribution

In Fig. 9(a), the distribution of internal particles was not uniform without preheating, which was observed not only in the far end, but also in the middle. Figure 9(b) shows the distribution of particles at both proximal and distal ends when the preheating temperature of particles was 1,100 °C. By calculation, S reduced from 2.97 to 2.90. This is because low preheating temperature produces greater cooling and influences the mixture of liquidity which affected the complete forming of anti-wear parts. High preheating temperature is beneficial to the combination of infiltration between particles and metal matrix, forming good bond strength. However, the

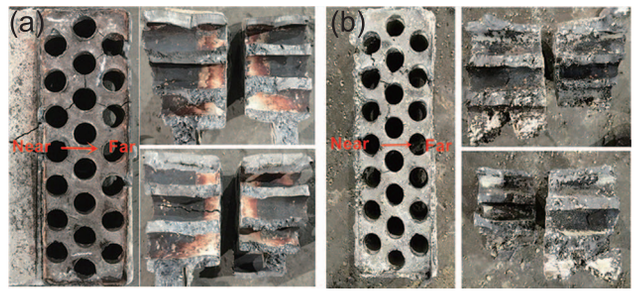

Fig. 9: Effect ofpreheating temperature on squeeze casting composite anti-wear parts: (a) 0 °C; (b) 1,100 °C

particles conglutination phenomenon can be observed when the preheating temperature was higher than 1,100 °C before mixing. In general, when the mixing temperature increases, the mixture becomes more liquid and gas is more easily discharged.

3.3 Effect of gate size (ΔA_{sur}) on particle distribution

In the above mixed regulation model, it is concluded that the smaller ΔA_{sur}, is, the smaller the change of runner cross-sectional area and the more favorable the mixing are. Therefore, by increasing the slope of the upper die by 5 °, the suddenly increase of the direct runner (shown in Fig. 10) is transformed into a gradually increased "horn" structure, and the corresponding ΔA_{sur} becomes smaller. Preparation of composite parts under the conditions of the above-mentioned optimized parameters (ejection speed of 150mm·s^{-1}, particle preheating temperature of 1,100 °C, pouring temperature of 1,600 °C). Through the comparison of Fig. 11, it can be seen that the particles appear in the distal near-middle region. The horn runner was beneficial to the uniform distribution of the near-end. According to the calculation of the particle distribution in, S is reduced from 3.15 to 2.81.

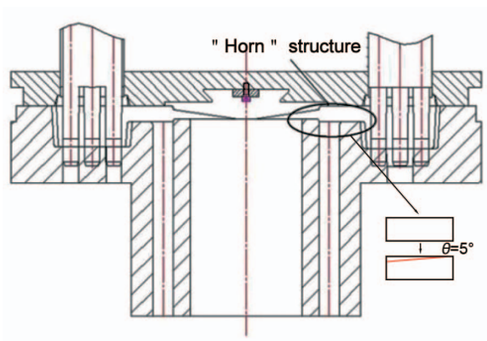

Fig. 10: Modified sprue structure "Horn"

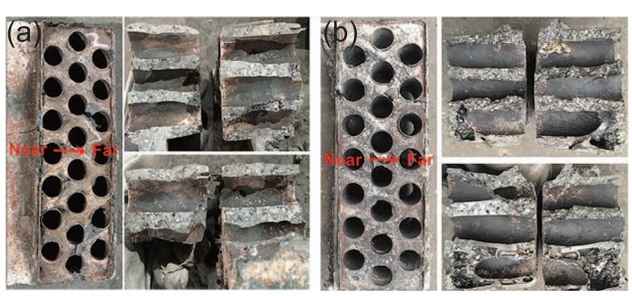

Fig. 11: Effect of gate size on squeeze casting composite parts: ΔA_{sur} (a) > (b)

4 Interface microstructure

The microstructure of interface between matrix and ceramic particles is shown in Fig. 12. It can be observed with the interface bonding state more clearly. It is found that the particles and the matrix form a "Class I interface" (the metal and reinforcements are neither reflected nor dissolved, and the interface is relatively flat) under the experimental parameters in Table 4, which is only mechanical and physical adhesion. This is because the molten metal is non-wetting with ZTA ceramic particles. Under the pressure compositing, the liquid metal is immersed in the rough surface of the ceramic particles to form a mechanical meshing interface on the micro scale which cannot be formed at atmospheric pressure. At the same time, the high temperature preheating of the particles before the mixing improves the activation degree of the particle surface, and also promotes the combination of the interface.

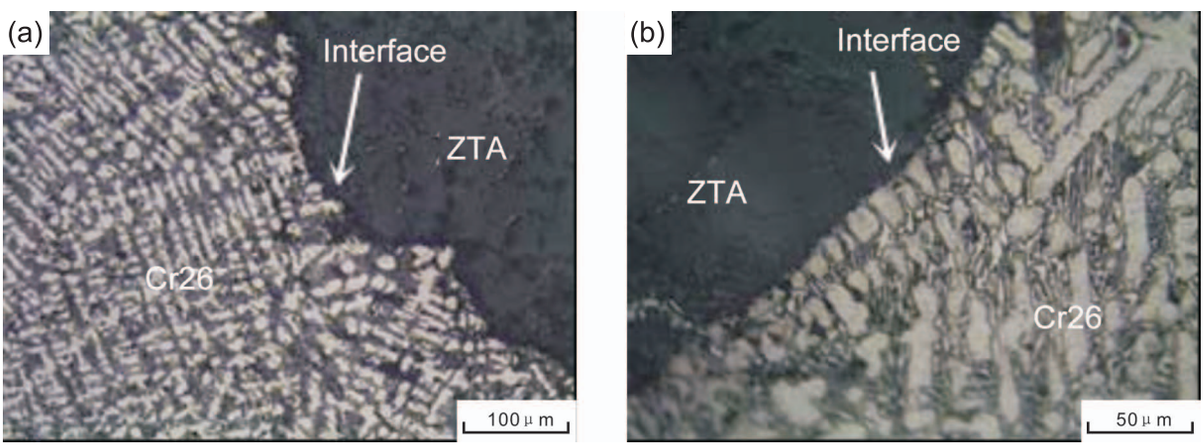

Fig. 12: Microstructure of interface between matrix and ceramic with different magnification

Table 4: Main technological parameters

Technological parameter	Data range
Fill pressure cylinder pressure	500 t
Pressure holding time	12 s
Ejection speed	150 mm·s^{-1}
Particle preheating temperature	1,100 °C
Pouring temperature	1,600 °C

5 Conclusions

(1) Mixed regulation models of ceramic particles with molten steel were proposed. It is concluded by analysis that the higher the temperature of ceramic particles T_p, the greater the molten metal speed V_m, and the smaller the A_{sur} was facilitated in mixing.

(2) By the shoot mixing process in SM-PC experiments, when the ejection speed was 150 mm·s^{-1}, preheating temperature of particles was 1,100 °C, and the shape of the runner was trumpet, the optimal particle distribution composite parts was obtained.

(3) The composite parts prepared by pressure compositing process in SM-PC achieved strong interface bonding between the metallic matrix and particles without wettability pretreatment.

References

[1] Lee H L, Lu W H, Chan S L. Abrasive wear of powder metallurgy Al alloy 6061-SiC particle composite. Wear,1992,159: 223–231.
[2] Kumar S. Effect of reinforcement size and volume fraction on the abrasive wear behavior of Al7075/ SiCpP/M composite-A statistical analysis. Tribology International, 2010, 43 : 414–422.
[3] Mahdavi S, Akhlaghi F. Effect of the SiC particle size on the dry sliding wear behavior of SiC and SiC-Gr-reinforced Al6061 composites. J Mater Sci, 2011, 46: 7883–7894.
[4] Zhao S M, Zhang X M, Zheng K H. Study on preparation and wear properties of ZTA/ high chromium cast iron matrix composites. Foundry Technology, 2011,32(12): 1673–1676. (In Chinese)
[5] Mondal D P, Das S. High stress abrasive wear behavior aluminum hard particle composite: effect of experimental parameters, particle size and volume fraction. Tribology International, 2006, 39: 470–478.
[6] He Xiaogang, Lu Dehong, Chen Shimin, et al. Preparation and thermal shock properties of Al2O3p/40Cr functionally graded composites materials. Source. Applied Mechanics and Materials, 2013,v 328: 901–905.
[7] Sree Manu K M, Sreeraj K, Rajan T P D, et al. Structure and properties of modified compocastmicrosilica reinforced aluminum matrix composite. Materials and Design, 2015, v 88: 294–301.
[8] Dhanashekar M, Kumar V S S. Squeeze casting of aluminum metal matrix composites-an overview. Procedia Engineering, 2014, v 97: 412–420.
[9] Edelbauer J, Schuller D, Lott O. High Temperature Squeeze Casting of Nickel Based Metal Matrix Composites with Interpenetrating Micro-structure. Materials Science Forum, 2015, (825–826): 93–100.
[10] Kish O, Froumin N, Aizenshtein M. Interfacial Interaction and Wetting in the Ta2O5/Cu-Al System. Journal of Materials Engineering and Performance, 2014, 23(5): 1551–1555.
[11] Wu Haobo, Zeng Fanhao, Yuan Tiechui. Wettability of 2519Al on B4C at 1000–1250 °C and mechanical properties of infiltrated B4C-2519Al composites. Ceramics International, 2014 ,40(1): 2073–2081.
[12] Mengyan H, Chen Weiping, Yang Shaofeng. Ni-induced non -pressure infiltration of stainless steel/Al203 ceramic composites. Special-cast and Non-ferrous Alloys, 2010, 30(8): 753–758. (In Chinese)
[13] Xing S M, Qiu B, Bao P W. A kind of preparation method of composite wear-resistant parts: China Patent, 201410745937.1. 2015-3-25.
[14] Hao Shiming, Jiang Min, Li Hongxiao. Material Thermodynamics, Beijing: Chemical industry press, 2010. (In Chinese)

This work was financially surpported by Central Universities under Grant (No.2018YJS139).